Growth mechanism of diamond by laser ablation of graphite in oxygen atmosphere

Z. Y. Chen, J. P. Zhao, T. Yano, and J. Sakakibara
Shikoku National Industrial Research Institute, Takamatsu 761-0395, Japan
(Received 1 February 2000; revised manuscript received 16 May 2000)

In this paper, diamond crystals grown on sapphire (0001) substrate by laser ablation in oxygen atmosphere were reported. The experiments were performed at a substrate temperature of ~550 °C and in oxygen pressure of 0.11–0.15 Torr. Field-emission scanning electron microscope (FE-SEM), x-ray diffraction (XRD), and micro-Raman spectroscopy were applied to characterize the products. FE-SEM observation revealed that hexagonal- and triangular-shaped crystals were formed on the sapphire substrate, however, the crystal nucleation and growth were nonuniform and discontinuous. XRD and micro-Raman analyses indicated the coexistence of hexagonal and cubic diamond. Moreover, the secondary nucleation of diamond was observed. The diamond growth mechanism in laser ablation, a physical vapor deposition process, was different than that in chemical vapor deposition process. In an optimum region of carbon energy, carbon species implanted into substrate to form a local high-density region in which the formation of diamond phase (sp^3 bond) rather than graphitic phase (sp^2 bond) was favorable. At suitable substrate temperature and oxygen pressure, the diamond crystals nucleated and grew, while the graphitic phases were excluded by oxygen preferential etching. Compared to diamond synthesized in a hydrogen environment, the conditions for diamond growth in oxygen atmosphere are very critical.

I. INTRODUCTION

Following the successful synthesis of diamond by high-pressure methods in the 1950's, the startling development of low-pressure synthesis of diamond films in the 1970's and 1980's almost immediately engendered great expectations of utility.[1] The last decade and a half have been an explosive growth in the synthesis of diamond materials by a variety of chemical vapor deposition (CVD) processes.[2] Small crystals (microns in size) and continuous polycrystalline thin films with several millimeter thick and over 12 in. (30 cm) in diameter are a reality.[2] Nowadays, the basic science of diamond growth by CVD is well understood. Typical CVD deposition of diamond is from a flowing gas mixture comprised of a small amount of methane (typically less than 1 at. %) in hydrogen at 10–50 Torr, activated with a hot filament (~2200 °C) or plasma near a substrate heated to between 700 and 1100 °C.[3,4] In diamond growth models, atomic hydrogen has been generally believed to play a central role in the various CVD processes, which had been said to stabilize the diamond lattice and to remove graphitic nuclei because of the preferential etching or regasification of graphite over diamond.[5]

Parallel to the development in the CVD technique of diamond, kinds of physical vapor deposition (PVD) techniques have been attempted to synthesize diamond in which carbon is supplied from solid targets. However, these methods only produce diamondlike carbon (DLC) with various content of sp^3 bond. Although sputtering, laser ablation, and filtered vacuum arc deposition have been attractive to synthesize DLC with sp^3 bond content up to 90%, this kind of DLC, called tetrahedral amorphous carbon, exhibits highly amorphous characteristics. So far, it is very difficult to synthesize diamond using PVD methods and only a few results on the growth of diamond particles by sputtering and laser ablation were reported.[6–8]

Very recently, Yoshimoto *et al.*[9] have reported the nucleation and growth of diamond on sapphire (0001) wafer by pulsed laser deposition (PLD) method. In their experiment, pure oxygen, instead of hydrogen commonly used in CVD diamond, was applied to etch graphitic carbon species. By choosing a temperature range that results in preferential oxidation of nondiamond (graphitic) carbon species to that of diamond, the accumulation of diamond was achieved. They found that diamond crystals could be grown at the substrate temperature of around 600 °C under oxygen pressure ranging from 0.1 to 0.2 Torr. In this paper, we will present new experimental results on the PLD diamond growth in oxygen atmosphere. Moreover, the aim of this paper attempts to understand the mechanism of diamond growth by PLD in oxygen environment and the effects of experimental parameters on the diamond nucleation and growth.

II. EXPERIMENT

The growth of diamond was conducted in a pulsed laser deposition chamber with a base pressure of less than 10^{-6} Torr. A KrF excimer laser (wavelength, 248 nm; pulse duration, 20 ns) was operated at 5 Hz, and the laser beam was impinged on a graphite target (randomly oriented pyrolytic graphite, 99.95% purity) at an off-normal angle of 45°. Synthetic sapphires with (0001) face were used as substrates for diamond growth. The substrate was positioned parallel to the laser incident direction at a distance of ~4 cm away from the target. High purity (99.999%) of oxygen was introduced into the chamber before deposition. All depositions were processed for 4 h at a constant laser power density of 10^8 W/cm^2 under the substrate temperature of ~550 °C and the oxygen pressure ranging from 0.11 to 0.15 Torr.

Products were characterized by field-emission scanning electron microscopy (FE-SEM: Hitachi, Model S-54001),

 ©2000 The American Physical Society

x-ray diffraction (XRD: RINT1200), and micro-Raman spectroscopy. Raman spectra were collected using a integrated fiber coupled Raman system consisting of a Nd:YAG (yttrium aluminum garnet) laser operated at 532 nm and 10 mW and an 1152×298 EEV MPP CCD chip in a Princeton Instrument thermoelectrically cooled camera. A laser beam of 16-μm spot size was focused onto the samples.

III. RESULTS

A. Field-emission scanning electron microscopy

Figure 1 shows FE-SEM images of a sample prepared at a substrate temperature of 550 °C under an oxygen pressure of 0.15 Torr. Figures 1(a), 1(b), and 1(c) were obtained from different regions of the sample, respectively. The nonuniform and discontinuous nucleation was clearly observed. The well-faceted particles have crystalline shapes, mostly being hexagonal and triangular. The largest particles were found to be about 1 μm, however, most of the particles are on the order of submicrometer to tens nanometer in diameter varying with different regions, as seen in Figs. 1(a) and 1(b), respectively. The nucleation density is about 10^7-10^8 cm^{-2}. The orientation of the sapphire (0001) substrate with a hexagonal structure is insetted in Fig. 1(c). Besides a few crystals, most of the hexagonal-shaped crystals nucleated and grew with an in-plane arrangement, which are azimuthally aligned with the $[1\bar{1}00]$ direction of sapphire. This is the same as the observation of Yoshimoto *et al.*[9]

B. X-ray diffraction

Figure 2 shows XRD pattern of the same sample shown in Fig. 1. As seen in Fig. 2(a), two sharp peaks resulted from the sapphire substrate and another two peaks with less intensity and relatively large full width half-maximum (FWHM) at 41.43° and 44.10°, were clearly observed. In order to exclude the diffraction pattern of the sapphire substrate, XRD measurement was carried out again as the sample was tilted a small angle to the incident direction of x ray. As shown in Fig. 2(b), XRD pattern only contains the information of the sample. The measured interplanar spacings (d) of this sample are given in Table I, where they are compared to the reported experimental values of cubic diamond, lonsdaleite, and the calculated values of 4H-, 6H-, 8H-, and 10H-hexagonal diamond. The interplanar spacings of the sample are very close to those values of lonsdaleite, 4H-, 8H-, and 10H-hexagonal diamond given in Table I, and one of them is close to that of cubic diamond and 6H-hexagonal diamond, respectively. The agreement between the *d* values of the sample and those reported is within the experiment error, less than 1%. In addition, no reflection was observed for the graphite (002) plane (3.66 Å) and (100) plane (2.13 Å). Thus, it can be concluded that the crystals are mainly hexagonal diamond and the presence of cubic diamond could not be excluded from the XRD results. However, the exact hexagonal structure was difficult to be determined according to the XRD pattern. Hexagonal diamond was formed in the work of Bundy and Kasper[10] during synthesizing conventional cubic diamond at high temperature and high pressure. This type of

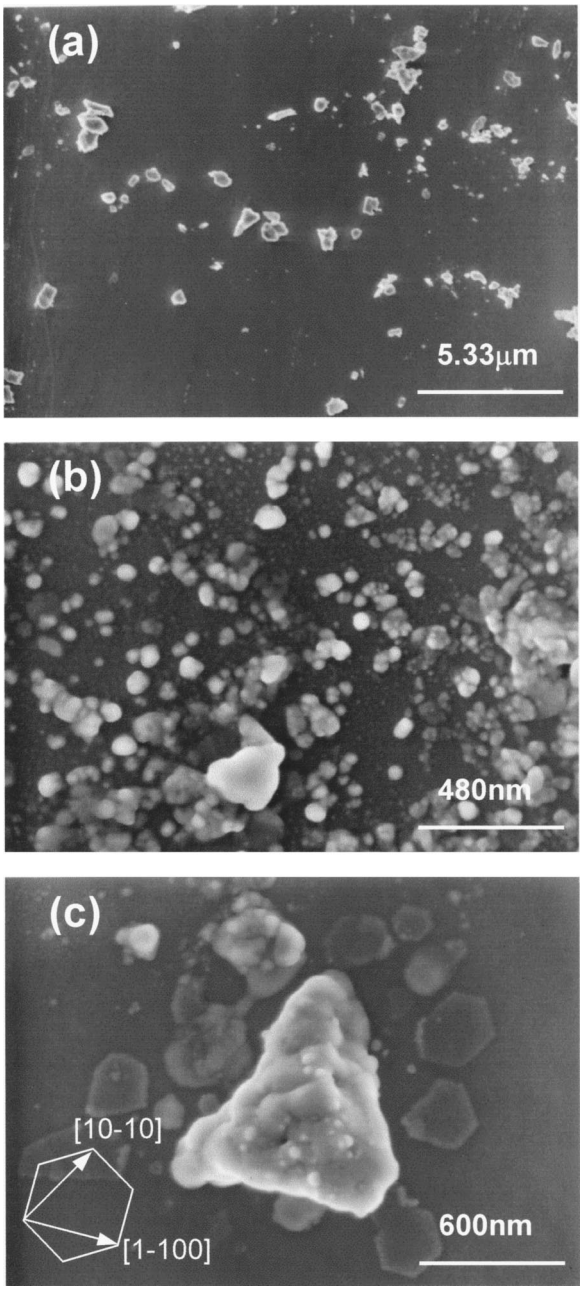

FIG. 1. FE-SEM micrographs of diamond crystals synthesized on sapphire (0001) substrate at a temperature of ~550 °C and an oxygen pressure of 0.15 Torr. (a), (b), and (c) are obtained from different regions of the sample, respectively. The orientation of sapphire (0001) substrate is inserted in (c), which has a hexagonal structure.

''shock-compressed'' diamond had previously been found only in meteorite.[11] Around 1990, hexagonal diamond was synthesized by weak shock loading,[12] low-pressure and low-temperature radio-frequency plasma-enhanced CVD,[13] hydrogen plasma jet,[14] and microwave plasma CVD.[15] However, no synthesis of hexagonal diamond using laser ablation method has been reported. It should be noted that the XRD pattern indicative of the presence of the hexagonal diamond observed in our paper was not found in the report of Yoshimoto *et al.*,[9] although similar experimental conditions were used in these two works. This may be attributed to the very close interplanar spacing between (100) hexagonal dia-

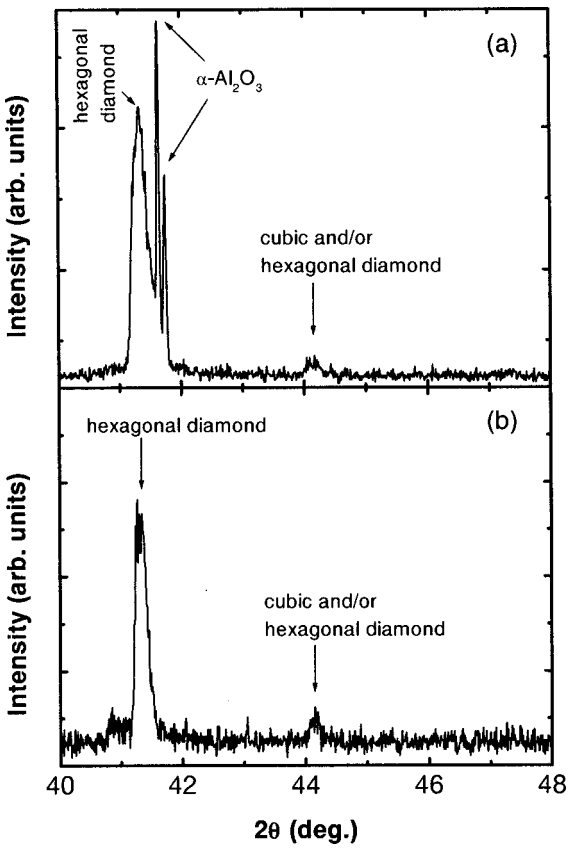

FIG. 2. XRD pattern of the sample shown in Fig. 1. The curve in (b) shows the XRD pattern obtained as the sample was tilted a small angle to incident direction of X ray.

mond and (0001) sapphire substrate. In this case, the diffraction from the hexagonal-diamond crystals with weak intensity is very likely to be masked by the strong diffraction from sapphire.

C. Micro-Raman spectroscopy

Raman studies of the crystals also demonstrated the existence of different forms of diamond: hexagonal and cubic.

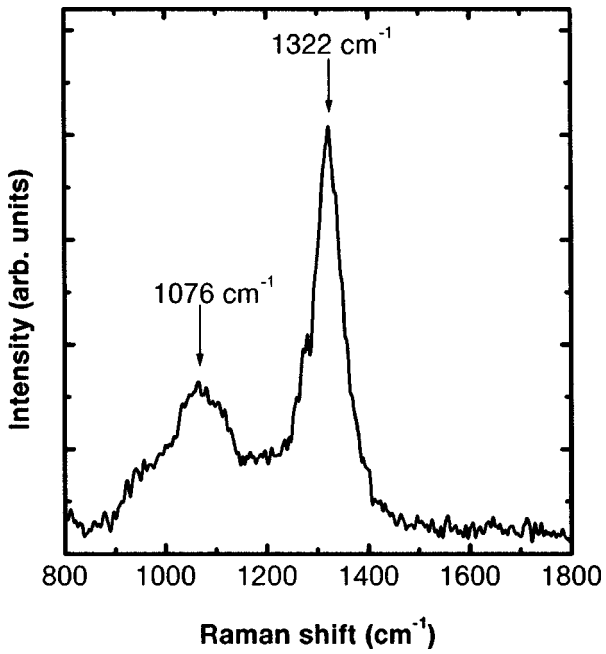

FIG. 3. Micro-Raman spectrum of the diamond crystal synthesized on sapphire (0001) substrate at a temperature of ~550 °C and an oxygen pressure of 0.15 Torr.

The Raman spectrum of the same sample from which the SEM and the x-ray data were obtained is shown in Fig. 3. A Raman peak at about 1322 cm^{-1} and a broad band at around 1076 cm^{-1} are observed simultaneously. We know that one phonon scattering in single-crystal diamond is dominated by a single intense peak at 1332 cm^{-1}, with FWHM of a few wave numbers. The sharp, characteristic peak is due to the periodicity of the lattice, which gives rise to a momentum selection rule. The micro-Raman spectrum that was observed by Yoshimoto *et al.*,[9] exhibited only one peak centered at 1332.8 cm^{-1} with FWHM of 3.4 cm^{-1}, which is very close to the perfect position of cubic diamond. In our case, a little shift of this peak from its perfect position of 1332 cm^{-1} down to 1322 cm^{-1} is observed. Moreover, its FWHM is found to be ~60 cm^{-1}, much broader than that of single-

TABLE I. Interplanar spacings (in angstrom) of diamond observed by x-ray diffraction measurement and reported in powder diffraction files.

Sample[a]	Cubic $a=3.57$ 6–0675[b]	2H-lonsdaleite $a=2.52$, $c=4.12$ 19–0268[b]	4H-hexagonal $a=2.52$, $c=8.24$ 26–1078[c]	6H-hexagonal $a=2.52$, $c=12.36$ 26–1082[c]	8H-hexagonal $a=2.52$, $c=16.47$ 26–1075[c]	10H-hexagonal $a=2.52$, $c=20.59$ 26–1081[c]
2.182		2.190 (100)	2.184 (100)		2.184 (100)	2.184 (100)
						2.172 (101)
					2.165 (101)	
				2.151 (101)		
						2.137 (102)
			2.111 (101)		2.111 (102)	
						2.081 (103)
2.052	2.060 (111)	2.060 (002)	2.059 (004)	2.059 (102)	2.059 (008)	2.059 (00 10)

[a]X-ray diffraction result shown in Fig. 2.
[b]JCPDS card No.
[c]JCPDS card No. (calculated).

crystal diamond. The downshift of the Raman peak and its broadened FWHM could be attributed to the nanosized diamond crystals as observed from SEM. In single-crystal IIa, diamond irradiated with 4 MeV carbon ions, Hunn *et al.* revealed that with increasing implantation damage, the triple degenerate one-phonon Raman mode at 1332 cm^{-1} broadened and shifted down to $\sim$1300 cm^{-1}.[16] Prawer *et al.*[17] found a downshift of the diamond peak to 1316 cm^{-1} for type IIa diamond implanted with 3.5-MeV He, and the damaged clusters were of the order of 1–2 nm in diameter.[18] They attributed the downshift of the diamond peak to the damage introduced by ion implantation, i.e., randomly displacing atoms from their crystal lattice site that changes the local bonding structure and results in the loss of long-range order. In addition, Prawer *et al.*[17] have recorded a strong peak at 1100 cm^{-1} in the Raman spectrum of diamond nanocrystals with a diameter of 5 nm.

The observed broad band at 1076 cm^{-1} is consistent with that proposed for nanocrystalline diamond.[17] Its position is close to the main peak of the vibrational density-of-states calculated by Beeman *et al.*[19] for the cluster model of diamond. Features around this position have already been attributed to ''microcrystalline diamond'' by Nemanich *et al.*[20] in CVD carbon films. They postulated that microcrystalline hexagonal diamond should give its strongest vibrational Raman frequency at 1175 cm^{-1}.[20] In the report by Maruyama *et al.*[14] on hexagonal diamond, a Raman response was shown at $\sim$1150 cm^{-1}. In this paper, considering the small crystal size, which might cause a downshift of Raman response and also broaden Raman peak, similar to that at 1332 cm^{-1} for cubic diamond, the observed broadband at 1076 cm^{-1} could be ascribed to nanocrystalline hexagonal diamond. We noted that the Raman band indicating the presence of the hexagonal diamond was not observed in Ref. 9, which is in agreement with the different XRD results obtained in these two works.

It is noted that the intensity of the broad Raman band at 1076 cm^{-1} is much less than that of the Raman peak at 1322 cm^{-1}. The possible formation of diamond polytypes weakens the Raman-scattering intensity[21] and contributes to the difficulties of Raman analysis. It is known that the Raman response of lonsdaleite (2H-hexagonal diamond) is many times smaller than that of cubic diamond, and that the Raman response of the latter is more than 50 times smaller than that of graphite.[22] A more stringent sample having large crystal size with high-nucleation density and known polytype is required for Raman analysis of the hexagonal diamond.

IV. DISCUSSION

As we known, the mechanism of diamond growth in CVD process has been well understood.[23] Compared with CVD diamond, the prevailing atomic arrangement in the carbon materials obtained by PVD process is amorphous or quasiamorphous with all possible combinations of sp, sp^2, and sp^3 bonds, even for the film deposited under hydrogen atmosphere. One possible reason may be due to the lower temperature presented in PVD process. Substrate temperature is another important parameter in diamond CVD besides atomic hydrogen. However, in PVD process, to promote substrate temperature gives rise to the transformation of carbon-carbon bonding from sp^3 to sp^2 forms, and results in the formation of graphitic phase, even for highly tetrahedrally bonded carbon film.[24]

In our paper, diamond crystals have been synthesized by laser ablation in oxygen atmosphere. This means a different growth mechanism compared with those in diamond CVD and DLC PVD processes. In the supplantation model,[25–27] the mechanism promoting sp^3 bonding over the normally more stable sp^2 bonding for amorphous carbon is related to shallow implantation of carbon ions with low energy (20–500 eV). In our case, the energy of the carbon ions generated from the graphite target by laser ablation is about 100 eV. According to the supplantation model, these energetic carbon ions will penetrate into the subsurface layers of substrate. The increase of local concentration of the penetrating carbon ions in substrate results in a local high-density region in which the local compressive stress reorders carbon atoms to form sp^3 bonds. The local high pressure might even take the material into a diamond-stable region of the carbon phase diagram.[28]

After supplantation, the hyperthermal carbon species will transfer their energy to the substrate atoms, and also lose their excess energy by participating in the collision cascade in a very short time ($\sim 10^{-13}-10^{-11}$ s). Therefore, the impingement of carbon particles creates immobile carbon interstitials at substrate temperature lower than 70 °C,[25] resulting in an amorphous carbon film. Once the amorphous carbon film forms, the crystallization to diamond is very difficult. Through post-deposition annealing, graphitization occurs rather than diamond-phase crystallization.[25,29–31] Therefore, in order to promote the formation of sp^3 long-range order, actually diamond crystal growth, a high-substrate temperature during deposition is necessary. Here, diamond crystals were synthesized at the substrate temperature of $\sim$550 °C. At such high-substrate temperature we can expect that three transforming processes coexist: diamond phase (sp^3 bond) crystallization, transformation of sp^3 bonding into sp^2 bonding, and graphitization. Clearly, a competitive growth between the diamond phase and the graphitic phase exists in our diamond growth process. To exclude or inhibit graphitic phase during diamond growth, another mechanism should be introduced.

It is well known that hydrogen is a decisive factor in CVD diamond growth by preferentially etching graphitic and amorphous carbon constituents. However, as mentioned above, hydrogenated amorphous carbon will be formed when the hydrogen is introduced into PVD process. At high-substrate temperature, graphitization will occur even for hydrogen incorporated ta-C film.[31] Similar to hydrogen, oxygen also selectively etches graphitic phase and its etching ability is several times higher than hydrogen. Our experimental results indicate that the graphitic phase was effectively excluded by oxygen etching, and consequently diamond crystal was successfully retained. We noted that the synthesized diamond in oxygen atmosphere has very small crystal size, which is similar to the diamond growth from hydrogen-depleted microwave plasma CVD.[23]

Summarily, in the diamond growth by laser ablation under oxygen atmosphere, energetic carbon species will shallowly implant into substrate surface where a local high-

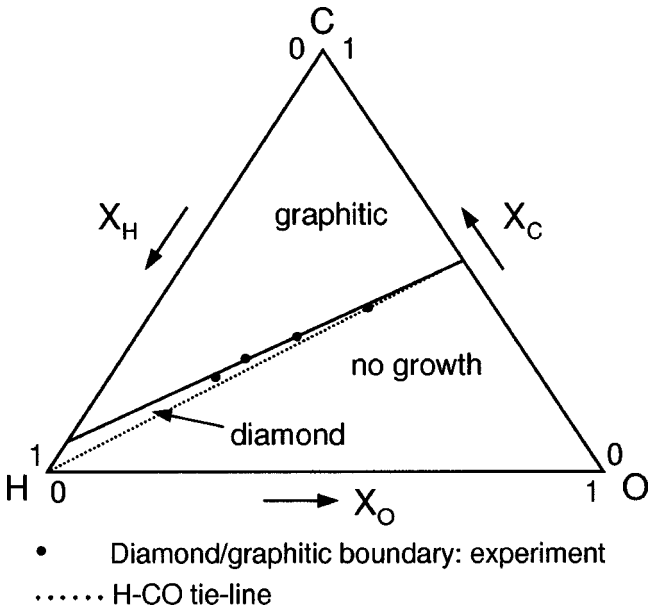

FIG. 4. Phase diagram for carbon-film deposition, showing experimental points on the diamond/graphitic domain boundary together with a boundary constructed from the phenomenological model described by Ford (Ref. 32). (After Ref. 33).

density area, favorable to form diamond phase, is generated. At a high-substrate temperature, the diamond phase nucleates and grows while the graphitic phase is preferentially etched by oxygen. In fact, a physical mechanism accompanying a chemical mechanism simultaneously induces diamond growth in this process.

Our experiment indicated the possibility of growing diamond by using the PVD process. However, the diamond crystals that we obtained have smaller size and lower nucleation density than CVD diamond. Moreover, the crystal growth is discontinuous and nonuniform. This implies that the growth parameters selected for PVD diamond are much stricter than that for CVD diamond. Hyperthermal carbon species with an optimum kinetic energy are necessary to generate a maximum density region favorable to diamond phase growth. Substrate temperature is also one of the key factors. At a low-substrate temperature, an amorphous structure will evolve, while at a high temperature, the crystallization and graphitization of diamond phase occur simultaneously if without oxygen. By introducing oxygen, the graphitic phase will be excluded; however, the diamond phase will also be etched by active oxygen. Compared with graphitic phase, the etching rate for the diamond phase should be low, thus part of the diamond phase will be retained at last. Therefore, it will cause a low-nucleation density and result in a discontinuous and nonuniform growth. Furthermore, the oxygen pressure is crucial for diamond growth in the PVD process. Figure 4 illustrates a phase diagram for carbon film deposition in a C–H–O system.[32,33] It is clearly seen that the region for diamond growth in oxygen atmosphere is quite narrow. Deviating from a very limited region, either a graphitic phase is produced or no growth occurs. This has been well demonstrated by Yoshimoto *et al.*[9] Therefore, the very precise control of these parameters is quite crucial for diamond growth in the PVD process.

In addition, the substrate effect should be considered, which will affect the final structure and crystalline orientation of diamond. The most favorable substrate for epitaxial growth of diamond film is that of diamond.[25] The ''mold'' effect of the host matrix determines the possible site occupancies of the penetrating species, epitaxial growth, and/or preferred orientation of film.[25] In present paper, the single-crystal sapphire with (0001) face was used as the substrate. FE-SEM and XRD results indicate that cubic- and hexagonal-diamond crystals can be grown on the sapphire (0001) face. Some of the synthesized diamond crystals have a well in-plane epitaxial relationship with the sapphire (0001) face, as seen in Fig. 1(c). In the work of Yoshimoto *et al.*,[9] the diamond crystals grown on the sapphire (0001) substrate, preannealed at 1000 °C, have an in-plane epitaxial relationship of diamond $[1\bar{1}0]$//sapphire $[1\bar{1}00]$, while the diamond crystals grown on a sapphire (0001) substrate, without preannealing, did not achieve such in-plane arrangement. In our paper, the diamond growth on a 1000 °C annealed sapphire (0001) substrate was also conducted, however, the results similar to that on unannealed substrate were obtained by SEM, XRD, and micro-Raman analyses. This is different with that reported by Yoshimoto *et al.*[9] Nevertheless, sapphire with (0001) face supplies a mold for the growth of diamond crystal on it. Moreover, the results again demonstrated the importance of precise control of the parameters for diamond growth.

From Fig. 1(c), we noted that secondary nucleation occurred on the ready-formed diamond crystals. On the one hand, the secondary nucleation has been found in CVD diamond growth from a hydrogen-poor C_{60}/Ar or CH_4/Ar plasma.[23] In these cases, the species C_2, carbon dimer, becomes dominant in the plasma, and serves as diamond-growth species. The unattached carbon atom can react with other C_2 molecules from the gas phase to nucleate a new diamond crystallite. In fact, our experimental work on the optical emission spectra of a carbon plume produced by KrF laser ablation of a graphite target revealed that C_2 carbon dimer is the dominant species. On the other hand, according to the supplantation model, the subsequent C_2 species implanted into the ready-formed diamond crystal will trigger the critical nucleation of a tetrahedrally bonded (sp^3) new phase. The mold effect would be responsible for the easily secondary nucleation on the ready-formed diamond crystals.

V. CONCLUSIONS

The nucleation and growth of diamond by laser ablation in oxygen atmosphere was obtained on a sapphire substrate at a temperature of ~550 °C. The XRD and micro-Raman results indicated the coexistence of hexagonal and cubic diamond. However, compared with CVD diamond synthesized in hydrogen environment, the diamond crystals formed, in present paper, had the size in nanometer range and exhibited discontinuous nucleation and growth. In addition, the secondary nucleation of diamond was observed. The shallow implantation of the high-energetic carbon species into the substrate favorably results in the formation of a diamond phase (sp^3 bond) rather than a graphitic phase. At the opti-

mal substrate temperature and oxygen pressure, the diamond crystal nucleated and grew, while the graphitic phase was excluded effectively by oxygen preferential etching. Results indicated that the very precise control of the experimental parameters and the mold effect of sapphire substrate are critical for diamond growth in the PVD process.

ACKNOWLEDGMENTS

The authors wish to thank Professor N. Nishida for providing access to FE-SEM. Z.Y.C. and J.P.Z. would like to thank the financial support provided by NEDO and JST Japan.

[1] D. M. Gruen and L. Buckley-Golder, MRS Bull. **23**, 16 (1998).
[2] J. E. Butler and H. Windischmann, MRS Bull. **23**, 22 (1998).
[3] *Proceedings of the 1st Conference on New Diamond Science and Technology*, edited by S. Saito, O. Fukunaga, and M. Yoshikawa (KTK Scientific/Terra Scientific, Tokyo, 1988).
[4] A. R. Badzian and R. C. DeVries, Mater. Res. Bull. **23**, 385 (1988).
[5] J. C. Angus and C. C. Hayman, Science **241**, 913 (1988).
[6] D. S. Olson, M. A. Kelly, S. Kapoor, and S. B. Hagstrom, J. Appl. Phys. **74**, 5167 (1993).
[7] E. B. D. Bourdon, P. Kovarik, and R. H. Rrince, Diamond Relat. Mater. **2**, 425 (1993).
[8] A. Rengan, N. Biunno, J. Narayan, and P. Moyer, Mater. Res. Soc. Symp. Proc. **162**, 185 (1990).
[9] M. Yoshimoto, K. Yoshida, H. Maruta, Y. Hishitani, H. Koinuma, S. Nishio, M. Kakihana, and T. Tachibana, Nature (London) **399**, 340 (1999).
[10] F. P. Bundy and J. S. Kasper, J. Chem. Phys. **46**, 3437 (1967).
[11] R. E. Hanneman, H. M. Strong, and F. P. Bundy, Science **155**, 995 (1967).
[12] T. Sekine, M. Akaishi, N. Setaka, and K. Kondo, J. Mater. Sci. **22**, 3615 (1987).
[13] S. R. P. Silva, G. A. J. Amaratunga, E. K. H. Salje, and K. M. Knowles, J. Mater. Sci. **29**, 4962 (1994).
[14] K. Maruyama, M. Makino, N. Kikukawa, and M. Shiraishi, J. Mater. Sci. Lett. **11**, 116 (1992).
[15] M. Kitabatake and K. Wasa, J. Vac. Sci. Technol. A **6**, 1793 (1988).
[16] J. D. Hunn, S. P. Withrow, C. W. White, and D. M. Hembree, Jr., Phys. Rev. B **52**, 8106 (1995).
[17] S. Prawer, K. W. Nugent, and D. N. Jamieson, Diamond Relat. Mater. **7**, 106 (1998).
[18] S. Prawer and R. Kalish, Phys. Rev. B **51**, 15 711 (1995).
[19] D. Beeman, J. Silverman, R. Lynds, and M. R. Anderson, Phys. Rev. B **30**, 870 (1984).
[20] R. J. Nemanich, J. T. Glass, G. Lucovsky, and R. E. Shroder, J. Vac. Sci. Technol. A **6**, 1783 (1988).
[21] M. Frenklach, R. Kematick, D. Huang, W. Howard, K. E. Spear, A. W. Phelps, and R. Koba, J. Appl. Phys. **66**, 395 (1989).
[22] D. S. Knight and W. B. White, J. Mater. Res. **4**, 385 (1989).
[23] D. M. Gruen, MRS Bull. **23**, 32 (1998).
[24] C. A. Davis, G. A. J. Amaratunga, and K. M. Knowles, Phys. Rev. Lett. **80**, 3280 (1998).
[25] Y. Lifshitz, S. R. Kasi, J. W. Rabalais, and W. Eckstein, Phys. Rev. B **41**, 10 468 (1990).
[26] J. Robertson, Diamond Relat. Mater. **2**, 984 (1993).
[27] C. A. Davis, Thin Solid Films **266**, 30 (1993).
[28] R. Berman and F. Simon, Z. Elektrochem. **59**, 333 (1955).
[29] H. Tsai and D. B. Bagi, J. Vac. Sci. Technol. A **5**, 3287 (1987).
[30] J. F. Prins, Phys. Rev. B **31**, 2472 (1985).
[31] S. Sattel, T. Giessen, H. Roth, M. Scheib, R. Ramlenski, R. Brenn, H. Ehrhardt, and J. Robertson, Diamond Relat. Mater. **4**, 333 (1995); **5**, 425 (1996).
[32] I. J. Ford, J. Appl. Phys. **78**, 510 (1995); J. Phys. D **29**, 2229 (1996).
[33] A. M. Stoneham, I. J. Ford, and R. P. Chalker, MRS Bull. **23**, 28 (1998).